

The Effect of Body Acceleration on Two Dimensional Flow of Casson Fluid through an Artery with Asymmetric Stenosis

Sachin Shaw¹, P. V. S. N Murthy*¹ and S. C. Pradhan²

¹Department of Mathematics, Indian Institute of Technology Kharagpur, Kharagpur, India

²Department of Aerospace Engineering, Indian Institute of Technology Kharagpur, Kharagpur, India

Abstract: Two dimensional flow of a non-Newtonian fluid through an asymmetric stenosed artery is analysed under the influence of body acceleration with an external magnetic field on the flow field. The Casson fluid model is considered to characterize the non-Newtonian behaviour of the blood. The flow is assumed to be unsteady, laminar, two-dimensional, asymmetric and of pulsatile nature. The artery wall has been treated as an elastic (moving wall) cylindrical tube. The unsteady flow mechanics is influenced by externally imposed periodic body acceleration. An explicit finite difference scheme is applied to obtain the flow field. The effect of body acceleration, magnetic field on the flowing blood is analyzed and these results are presented through graphs for the axial and radial velocities, flow rate and wall shear stress.

Keywords: Casson fluid, periodic body acceleration, magnetohydrodynamics (MHD), asymmetric stenosis, moving wall.

INTRODUCTION

Atherosclerosis is a disease of large- and medium- size arteries which involve complex interactions between the artery wall and blood flow. Hemodynamics factors, such as wall shear stress levels, particle residence times, arterial wall shears and wall compliance play very important roles in maintaining normal vascular endothelial function which is directly related to the propagation and generation of the atherosclerotic lesion [1-3]. The actual reason for formulation of stenosis is not known, but its effect over the flow characteristics has been studied by many research workers [4, 5]. The formulation of stenosis, block the circulation of the blood in the heart which may cause of many cardiovascular diseases as myocardial infarction, angina etc. Externally imposed body acceleration also has major influence on the flow through the stenosed artery. In many situations in our life while fast body movements in sports activities, driving in fast moving vehicles we feel the body acceleration or vibration. Due to this body acceleration, different health problems such as headache, loss of vision, increase in pulse rate, abnormal pain etc occur. On the basis of experimental results, it is observed that the body acceleration, might change the heart beat, and might have a negative impact on the circulatory system. Chakravarty and Mandal [6] studied the pulsatile flow through the stenosed artery under the influence of the externally imposed body acceleration and discussed its influence on the circulatory system.

Quite a good number of analytical studies pertaining to the blood flow through stenosed arteries [7-10] analyzing the arterial construction on the flow through larger arteries at high rate exist in the literature, where in blood is as-

sumed to behave like a Newtonian fluid. Chakravarty and Mandal [10] analyzed the blood flow through a bifurcated stenosed artery. They have pointed out that away from the flow divider, the flow rate becomes higher due to the forward flow and gets reversed near the flow divider. While blood being a suspension of cells which behaves as a non-Newtonian fluid at low shear rates and during its flow through small blood vessels, and especially in diseased states when clotting effects in small arteries are presents [11-13]. Many experiments [12-18] were conducted on blood with varying hematocrit, anticoagulant, temperature, etc. suggested that at low shear rates, blood behaves as Casson fluid. Aroesty and Gross [12] have analyzed the pulsatile flow of blood vessels with application to microcirculation. Dash and Mehta [16] have investigated the Casson fluid flow through a pipe filled with porous medium. They noticed that the plug flow radius increases with increase in the value of yield stress and this increases wall shear.

In the bioengineering and medical technology, one of the promising methods to accomplish precise targeting is magnetic drug delivery [19] and cell separation [20] and extensive research work [21-26] has been reported on the flow dynamics in the presence of magnetic field. It was estimated that the magnetic susceptibility of blood be 3.5×10^{-6} and -6.6×10^{-7} for the venous and arterial blood respectively. Since the blood is an electrically conducting fluid, the magnetohydrodynamic (MHD) principle has been used to decelerate the flow of blood in human arterial system and treat of certain cardiovascular disorders. It is well established from the literature that a uniform transverse magnetic field can alter the flow rate of blood. Flow control is more important mainly to reduce bleeding during surgery [21]. It is also noticed that the heart rate decreases by exposing biological systems to an external magnetic field [27]. There are several studies [26, 28, 29], the results of which are useful in devising biomedical tools which are useful in proper treatment of blood trans-

*Address correspondence to this author at the Department of Mathematics, Indian Institute of Technology Kharagpur, Kharagpur, India;
Tel: 91-3222-283646; Fax: 91-3222-282700;
E-mail: pvsnm@maths.iitkgp.ernet.in

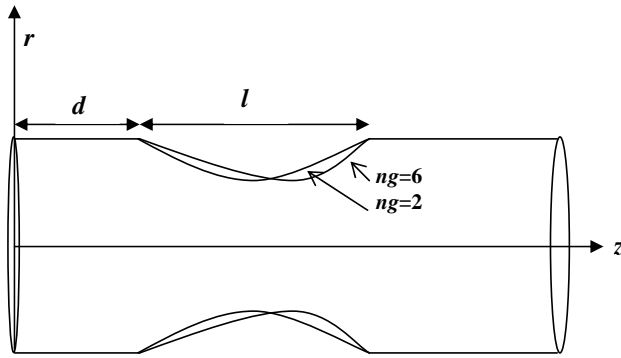


Fig. (1). Geometry of the artery with asymmetric stenosis.

port in tumor, brain tissue and soft connective tissue zones as well as in the stenosed artery. It is important to capture the drug particle near the stenosed portion in an artery particularly in a deceased cardiovascular system. Magnetic nanoparticles are mingled with drug particles and these particles are captured near the tumor using an external magnetic field. So it is important to analyze the flow behavior near the tumor to control the trajectory of the carrier particles [19, 20].

Mandal *et al.* [30] analyzed the effect of body acceleration on the power law fluid flowing through a symmetric stenosis. In this investigation we aim at analyzing the influence of the externally imposed body acceleration on the flow of blood through an asymmetric stenosed artery by considering blood as Casson fluid. The artery is cylindrical in shape and the flow is axially symmetric. Also it is aimed at exploring the influence of the externally imposed magnetic field on the non-linear Casson flow field.

MATHEMATICAL MODEL

Consider the unsteady, fully developed, axially symmetric, laminar 2D pulsatile flow in presence of external imposed periodic body acceleration in an arterial segment which is treated as a long tube having an asymmetric mild stenosis in its lumen. The following assumptions are made: All the physical properties are constant. The artery wall motion is introduced into the local fluid mechanics but not on the stresses and the strains on the vascular wall. The blood (fluid) is electrically conducting, and treated as Casson fluid. A uniform transverse magnetic field B_0 acts along the radial direction of the artery. The periodic body acceleration $\mathbf{F}(t)$ applied in the axial direction.

Let (r, θ, z) be the coordinates of the representative material point in the cylindrical polar coordinate system, where the z -axis is taken along the axis of the artery while (r, θ) are taken along the radial and the circumferential directions, respectively. The geometry of the artery (cf. Fig. 1) considering in the present investigation with a mild stenosis is represented as (Sankar *et al.* [31]),

$$R(z,t) = r_0 [1 - \eta \{ l(z-d)^{ng-1} - (z-d)^{ng} \}] a_1(t) \quad d \leq z \leq d+l \quad (1)$$

$$= r_0 a_1(t), \quad \text{otherwise}$$

where $\eta = \frac{h_m n_g^{ng-1}}{r_0 l^{ng} (ng-1)}$, where ng is the parameter representing the asymmetry of the stenosis, $ng=2$ represents that the

stenosis is symmetric. η represent the shape of the stenosis. l is the length of the stenosis, h_m is the maximum height of the stenosis, d is the distance of the stenosis from the inlet, r_0 being the unstricted radius of the stenosed vessel. The time-variant parameter $a_1(t)$ is given by

$$a_1(t) = 1 + k_R \cos(\omega_p t - \phi) \quad (2)$$

in which k_R is called the amplitude, which is a constant.

The continuity and the momentum equations for the tohydrodynamics (MHD) flow are written as:

$$\nabla \cdot \mathbf{V} = 0 \quad (3)$$

$$\frac{D\mathbf{V}}{Dt} = -\frac{1}{\rho} \nabla p + \nabla \cdot \boldsymbol{\tau} + \mathbf{J} \times \mathbf{B} + \mathbf{F}(t), \quad (4)$$

the periodic body acceleration $\mathbf{F}(t)$ in the axial direction is given by,

$$\mathbf{F}(t) = a_0 \cos(\omega_b t + \phi), \quad (5)$$

a_0 is its amplitude, $\omega_b = 2\pi f_b$, f_b is it's frequency in Hz, ϕ is its phase angle of $\mathbf{F}(t)$ with respect to the heart action. The frequency of the body acceleration f_b is assumed to be small, so that wave effects can be neglected. $\frac{D\mathbf{V}}{Dt}$ is the material

derivative, \mathbf{V} , the velocity $(u, 0, w)$, \mathbf{J} is the current density, p is the pressure, $\mathbf{B} = \mathbf{B}_0 + \mathbf{B}_1$ is the total magnetic field where \mathbf{B}_1 is the induced magnetic field which is negligible in comparison with the external magnetic field \mathbf{B}_0 which is justified for MHD flow at small magnetic Reynolds number. $\boldsymbol{\tau}$ is the shear tensor.

By Ohm's law, we have

$$\mathbf{J} = \sigma (\mathbf{E} + \mathbf{V} \times \mathbf{B}) \quad (6)$$

Where σ is the electrical conductivity and \mathbf{E} is the electric field. The imposed and induced electrical fields are assumed to be negligible. The force $\mathbf{J} \times \mathbf{B}$ can be simplified to

$$\mathbf{J} \times \mathbf{B} = -\sigma \mathbf{B}^2 \mathbf{V} \quad (7)$$

The governing equations for the z and r components of momentums with the equation of continuity in the cylindrical coordinate system due to magnetohydrodynamics (MHD) interactions, may be written as

$$\frac{\partial w}{\partial t} + u \frac{\partial w}{\partial r} + w \frac{\partial w}{\partial z} = -\frac{1}{\rho} \frac{\partial p}{\partial z} - \frac{1}{\rho} \left[\frac{1}{r} \frac{\partial}{\partial r} (r \tau_{rz}) + \frac{\partial}{\partial z} (\tau_{zz}) \right] - \frac{\sigma B_0^2}{\rho} w + F(t) \quad (8)$$

$$\frac{\partial u}{\partial t} + u \frac{\partial u}{\partial r} + w \frac{\partial u}{\partial z} = -\frac{1}{\rho} \frac{\partial p}{\partial r} - \frac{1}{\rho} \left[\frac{1}{r} \frac{\partial}{\partial r} (r \tau_{rr}) + \frac{\partial}{\partial z} (\tau_{rz}) \right] \quad (9)$$

$$\frac{\partial u}{\partial r} + \frac{u}{r} + \frac{\partial w}{\partial z} = 0. \quad (10)$$

Where $w(r,z,t)$ and $u(r,z,t)$ are the axial and radial components of the velocity, respectively.

At the wall, axial velocity is zero and the radial velocity is equal to the velocity of the artery wall which is due to the wall motion, and these conditions are represented as,

$$\begin{aligned} w(r, z, t) &= 0 \quad \text{on } r = R(z, t) \\ u(r, z, t) &= \frac{\partial R(z, t)}{\partial t} \quad \text{on } r = R(z, t). \end{aligned} \quad (11.a)$$

Along the axis of symmetry, axial velocity gradient and the radial velocity are zero,

$$\begin{aligned} \frac{\partial}{\partial r} w(r, z, t) &= 0 \quad \text{on } r = 0 \\ u(r, z, t) &= 0 \quad \text{on } r = 0. \end{aligned} \quad (11.b)$$

Initially ($t = 0$) the flow velocity in the presence of the magnetic field is considered as:

$$w(r, z, 0) = \left(\frac{A_0 + A_1}{M^2} \right) \left\{ 1 - \frac{I_0(Mr)}{I_0(MR)} \right\}, \quad u(r, z, 0) = 0, \quad (12)$$

where I_0 is the modified Bessel function of the first kind of order zero.

In the absence of the magnetic field, the above initial condition reduces to

$$w(r, z, 0) = \left(\frac{A_0 + A_1}{4k_c^2} \right) \left\{ 1 - \frac{r^2}{r_0^2} \right\}, \quad u(r, z, 0) = 0, \quad (13)$$

which represents the Hagen-Poiseuille flow.

Since the lumen radius is very small compared to the wavelength of the pressure wave, equation of motion in the radial direction reduced to $\frac{\partial p}{\partial r} = 0$, and hence equation (9) becomes $p = p(z, t)$ and the pressure gradient can be written as:

$$-\frac{\partial p}{\partial z} = A_0 + A_1 \cos(\omega_p t), \quad t > 0 \quad (14)$$

where, A_0 is the steady state part of the pressure gradient and A_1 is the amplitude of its oscillating part and $\omega_p = 2\pi f_p$, f_p being the heart pulse frequency.

Following Fung [10], the rheological equation of state for an isotropic, incompressible flow of a Casson fluid can be written as:

$$\tau_{ij} = 2\mu(J_2)e_{ij} \quad (15)$$

where $\mu(J_2) = (k_c J_2^{1/4} + 2^{-3/4} \tau_y^{1/2})^2 \cdot J_2^{-1/2}$

$$J_2 = \frac{1}{4} e_{ij} e_{ij} = \left\{ \left(\frac{\partial u}{\partial r} \right)^2 + \left(\frac{u}{r} \right)^2 + \left(\frac{\partial w}{\partial z} \right)^2 \right\} + \frac{1}{2} \left(\frac{\partial u}{\partial z} + \frac{\partial w}{\partial r} \right)^2 \quad (16)$$

$\mu(J_2)$, $J_2 = \frac{1}{4} e_{ij} e_{ij}$, τ_y and k_c^2 are the apparent viscosity, the rate of strain tensor invariant, yield stress and Casson's coefficient of viscosity respectively. δ_{ij} , τ_{ij} are the Kronecker delta and stress component, respectively. $e_{ij} = \frac{1}{2}(v_{ij} + v_{ji})$ is

the rate of strain tensor, where V_{ij} represents the shear rate defined as $v_{ij} = \frac{\partial v_i}{\partial r_j} + \frac{\partial v_j}{\partial r_i}$, v_i and r_i represents the velocity and coordinate, respectively. The flow conditions are given by

$$\begin{aligned} e_{ij} &= 0 & \text{if } J_2 < \tau_y^2 \\ &= \tau_{ij} / 2\mu(J_2) & \text{if } J_2 \geq \tau_y^2 \end{aligned} \quad (17)$$

The following non-dimensional variables are used, in the governing equations and the boundary conditions.

$$\begin{aligned} r^* &= \frac{r}{r_0}, z^* = \frac{z}{r_0}, u^* = \frac{u}{w_0}, w^* = \frac{w}{w_0}, p^* = \frac{p}{\rho w_0^2}, t^* = \frac{t w_0}{r_0}, \omega_p^* = \frac{\omega_p r_0}{w_0}, \omega_b^* = \frac{\omega_b r_0}{w_0} \\ \tau_{ij}^* &= \frac{\tau_{ij} r_0}{k_c^2 w_0}, \tau_y^* = \frac{\tau_y r_0}{k_c^2 w_0}, \nu = \frac{k_c^2}{\rho}, A_0^* = \frac{A_0 r_0}{\rho w_0^2}, A_1^* = \frac{A_1 r_0}{\rho w_0^2}, a_0^* = \frac{a_0 r_0}{\rho w_0^2} \end{aligned} \quad (18a)$$

where w_0 is the average velocity at the axial direction. The other parameter like the Reynolds number (Re) and the Hartmann number (M) are defined as:

$$Re = \frac{w_0 r_0}{\nu}, \quad M = \sqrt{\frac{\sigma B_0^2 r_0}{\rho w_0}} \quad (18.b)$$

The governing equations Eqns. (8) and (10) can be written in their non-dimensional form (ignoring the astrich '*) as:

$$\frac{\partial w}{\partial t} + u \frac{\partial w}{\partial r} + w \frac{\partial w}{\partial z} = -\frac{\partial p}{\partial z} - \frac{1}{Re} \left[\frac{1}{r} \frac{\partial}{\partial r} (r \tau_{rz}) + \frac{\partial}{\partial z} (\tau_{zz}) \right] - \frac{M^2}{Re} w + F(t) \quad (19)$$

$$\frac{\partial u}{\partial r} + \frac{u}{r} + \frac{\partial w}{\partial z} = 0 \quad (20)$$

where $\tau_{zz} = 2\mu(J_2) \left(\frac{\partial w}{\partial z} \right)$, $\tau_{rz} = 2\mu(J_2) \left(\frac{\partial u}{\partial z} + \frac{\partial w}{\partial r} \right)$

$$\begin{aligned} \mu(J_2) &= (J_2^{1/4} + 2^{-3/4} \tau_y^{1/2})^2 \cdot J_2^{-1/2} \quad \text{with } J_2 = \left\{ \left(\frac{\partial u}{\partial r} \right)^2 + \left(\frac{u}{r} \right)^2 + \left(\frac{\partial w}{\partial z} \right)^2 \right. \\ &\quad \left. + \frac{1}{2} \left(\frac{\partial u}{\partial z} + \frac{\partial w}{\partial r} \right)^2 \right\} \end{aligned} \quad (21)$$

Equations (1), (5) and (14) in its non-dimensional form look as:

$$R(z, t) = [1 - \eta \{ l(z-d)^{ng-1} - (z-d)^{ng} \}] a_1(t) \quad d \leq z \leq d+l \quad (22)$$

$$= a_1(t), \quad \text{otherwise}$$

$$F(t) = a_0 \cos(\omega_b t + \varphi) \quad (23)$$

$$\text{and } -\frac{\partial p}{\partial z} = A_0 + A_1 \cos(\omega_p t), \quad t > 0 \quad (24)$$

METHOD OF SOLUTION

Using the radial coordinate transformation $x = \frac{r}{R(z, t)}$ (25)

$$\frac{\partial w}{\partial t} = \left\{ \frac{x}{R} \frac{\partial R}{\partial t} \frac{u}{R} + \frac{x}{R} \frac{\partial R}{\partial z} w \right\} \frac{\partial w}{\partial x} - \frac{\partial p}{\partial z} w - \frac{\partial w}{\partial z} \frac{1}{\text{Re}} \left[\frac{1}{xR} \tau_{xz} + \frac{1}{R} \frac{\partial \tau_{xz}}{\partial x} + \frac{\partial \tau_{zz}}{\partial z} - \frac{x}{R} \frac{\partial R}{\partial z} \frac{\partial \tau_{zz}}{\partial x} \right] - \frac{1}{\text{Re}} M^2 w + F(t) \quad (26)$$

Equations (19) and (20) can be written as:

$$\frac{1}{R} \frac{\partial u}{\partial x} + \frac{u}{xR} + \frac{\partial w}{\partial z} - \frac{x}{R} \frac{\partial R}{\partial z} \frac{\partial w}{\partial x} = 0, \quad (27)$$

where

$$\begin{aligned} \tau_{xz} &= 2\mu(J_2) \left(\frac{\partial u}{\partial z} - \frac{x}{R} \frac{\partial R}{\partial z} \frac{\partial u}{\partial x} + \frac{1}{R} \frac{\partial w}{\partial x} \right), \\ \tau_{zz} &= 2\mu(J_2) \left(\frac{\partial w}{\partial z} - \frac{x}{R} \frac{\partial R}{\partial z} \frac{\partial w}{\partial x} \right) \\ \mu(J_2) &= (J_2^{1/4} + 2^{-3/4} \tau_y^{1/2})^2 \cdot J_2^{-1/2} \\ \text{with } J_2 &= \left(\frac{1}{R} \frac{\partial u}{\partial x} \right)^2 + \left(\frac{u}{xR} \right)^2 + \left(\frac{\partial w}{\partial z} - \frac{x}{R} \frac{\partial R}{\partial z} \frac{\partial w}{\partial x} \right)^2 + \frac{1}{2} \left(\frac{\partial u}{\partial z} - \frac{x}{R} \frac{\partial R}{\partial z} + \frac{1}{R} \frac{\partial w}{\partial x} \right)^2, \end{aligned} \quad (28)$$

and the boundary become:

$$\begin{aligned} w(x, z, t) = 0, \quad u(x, z, t) &= \frac{\partial R}{\partial t} \quad \text{at } x = 1, \\ \frac{\partial}{\partial x} w(x, z, t) = 0, \quad u(x, z, t) &= 0 \quad \text{on } x = 0. \end{aligned} \quad (29)$$

Multiplying continuity equation (27) by xR and integrating with respect to x ,

$$u(x, z, t) = x \frac{\partial R}{\partial z} w - \frac{R}{x} \int_0^x x \frac{\partial w}{\partial z} dx - \frac{2}{x} \frac{\partial R}{\partial z} \int_0^x x w dx. \quad (30)$$

This equation takes the following form using boundary condition (29) for u ,

$$-\int_0^1 x \frac{\partial w}{\partial z} dx = \int_0^1 x \left[\frac{2}{R} \frac{\partial R}{\partial z} w + \frac{1}{R} \frac{\partial R}{\partial t} f(x) \right] dx. \quad (31)$$

Since the choice of $f(x)$ is, of course, arbitrary, let $f(x)$ be of the form

$$f(x) = -4(x^2 - 1) \quad \text{satisfied} \quad \int_0^1 x f(x) dx = 1. \quad (32)$$

Taking the approximation of the equality between the integrals to integrands, we have from (31),

$$\frac{\partial w}{\partial z} = -\frac{2}{R} \frac{\partial R}{\partial z} w + \frac{4}{R} \frac{\partial R}{\partial t} (x^2 - 1). \quad (33)$$

Introducing (33) into (30) one gets,

$$u(x, z, t) = x \left[\frac{\partial R}{\partial z} w + \frac{\partial R}{\partial t} (2 - x^2) \right]. \quad (34)$$

Solving Equation (23) based on the central difference approximations for all the spatial derivatives in the following manner:

$$\begin{aligned} \frac{\partial w}{\partial x} &= \frac{w_{i,j+1}^k - w_{i,j-1}^k}{2\Delta x} = w_{fx} \\ \frac{\partial w}{\partial z} &= \frac{w_{i+1,j}^k - w_{i-1,j}^k}{2\Delta z} = w_{fz} \end{aligned} \quad (35.a)$$

while the time derivative is approximated by

$$\frac{\partial w}{\partial t} = \frac{w_{i,j}^{k+1} - w_{i,j}^k}{\Delta t} \quad (35.b)$$

Similar expression can also be obtained from other spatial derivatives. Here $w(x, z, t)$ is discretised to $w(x_j, z_i, t_k)$ and in turn to $w_{i,j}^k$ where we define $x_j = (j-1)\Delta x, (j = 1, 2, \dots, N+1)$ such that $x_{N+1} = 1.0$, $z_i = (i-1)\Delta z (i = 1, 2, \dots, L+1)$ and $t_k = (k-1)\Delta t, (k = 1, 2, \dots)$ for the entire segment. $\Delta x, \Delta z$ and Δt are the increment at the axial direction, radial direction and in time step, respectively.

So the equation (26) transformed into

$$\begin{aligned} w_{i,j}^{k+1} &= w_{i,j}^k + \Delta t \left[-\frac{1}{\rho} \left(\frac{\partial p}{\partial z} \right) + \left\{ \frac{x_j}{R_i^k} \left(\frac{\partial R}{\partial t} \right) - \frac{u_{i,j}^k}{R_i^k} + \frac{x_j}{R_i^k} \left(\frac{\partial R}{\partial z} \right) \right\} w_{i,j}^k \right] \\ &\quad - \frac{1}{\text{Re}} \left\{ \frac{1}{x_j R_i^k} (\tau_{xz})_{i,j}^k + \frac{1}{R_i^k} (\tau_{zz})_{i,j}^k + (\tau_{zz})_{i,j}^k - \frac{x_j}{R_i^k} \left(\frac{\partial R}{\partial z} \right) (\tau_{zz})_{i,j}^k - M^2 w_{i,j}^k \right\} + F^{k+1}, \end{aligned} \quad (36)$$

where $(\tau_{zz})_{i,j}^k = -2\mu(J_2) \left[(w_{fz})_{i,j}^k - \frac{x_j}{R_i^k} \left(\frac{\partial R}{\partial z} \right) (w_{fx})_{i,j}^k \right]$

$$(\tau_{xz})_{i,j}^k = -2\mu(J_2) \left[(u_{fz})_{i,j}^k - \frac{x_j}{R_i^k} \left(\frac{\partial R}{\partial z} \right) (u_{fx})_{i,j}^k + \frac{1}{R_i^k} (w_{fx})_{i,j}^k \right],$$

with $\mu(J_2) = (J_2^{1/4} + 2^{-3/4} \tau_y^{1/2})^2 \cdot J_2^{-1/2}$,

$$\begin{aligned} J_2 &= \left(\frac{1}{R_i^k} (u_{fx})_{i,j}^k \right)^2 + \left(\frac{u_{fz}^k}{x_j R_i^k} \right)^2 + \left((w_{fz})_{i,j}^k - \frac{x_j}{R_i^k} \left(\frac{\partial R}{\partial z} \right) (w_{fx})_{i,j}^k \right)^2 \\ &\quad + \frac{1}{2} \left((u_{fz})_{i,j}^k - \frac{x_j}{R_i^k} \left(\frac{\partial R}{\partial z} \right) (u_{fx})_{i,j}^k + \frac{1}{R_i^k} (w_{fx})_{i,j}^k \right)^2. \end{aligned} \quad (37)$$

And the corresponding boundary conditions,

$$w_{i,N+1}^k = 0, \quad u_{i,N+1}^k = \left(\frac{\partial R}{\partial t} \right)_i, \quad w_{i,1}^k = w_{i,2}^k \quad \text{and} \quad u_{i,1}^k = 0 \quad (38)$$

also the corresponding initial conditions are in the presence of magnetic field and in the absence of magnetic field is respectively, as

$$u_{i,j}^1 = \left(\frac{A_0 + A_1}{M^2} \right) \left\{ 1 - \frac{I_0(M x_j)}{I_0(M)} \right\} \quad (39.a)$$

$$u_{i,j}^1 = 2(1 - x_j^2). \quad (39.b)$$

Now with the help of radial and axial velocity, one can easily determined the volumetric flow (Q) and the wall shear stress (τ_w) from the following relations,

$$Q_i = 2\pi (R_i^k)^2 \int_0^1 x_j w_{i,j}^k dx_j \quad (40)$$

$$\tau_w^k = (\tau_{xz})_{i,j}^k \times \cos \left[\arctan \left(\frac{\partial R}{\partial z} \right) \right] \quad (41)$$

RESULT AND DISCUSSION

The following values of the parameters are considered in the study which have a major physiological significance in the cardiovascular system, $[20-22]$, $r_0 = 800 \mu m$, $A_0 = 100 \text{ kg m}^{-2} \text{ s}^{-2}$, $A_1 = 0.2A_0$, $d = 0.025 \text{ m}$, $l = 0.015 \text{ m}$, $k_c^2 = 0.035 \text{ P}$, $\omega_b = 0.02$, $\omega_p = 0.02$, $a_0 = 0.1$, $k_R = 0.05$, $\rho =$

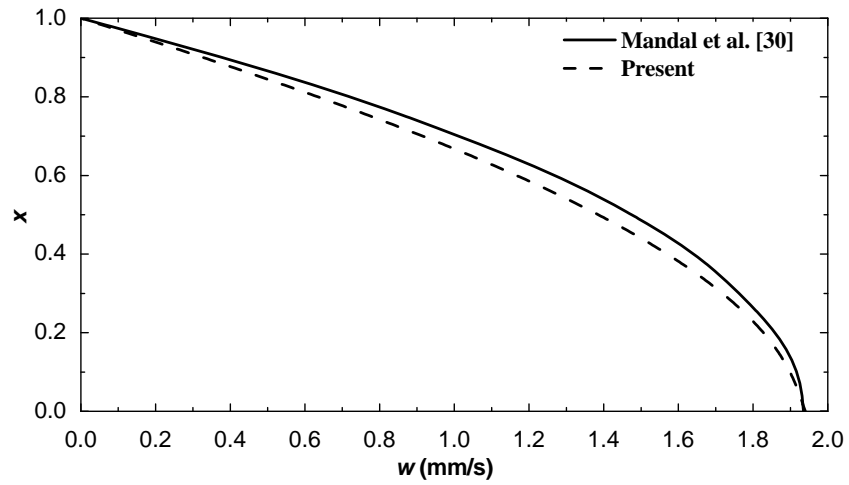


Fig. (2). Axial velocity .vs. radial coordinate x for Newtonian fluid $\phi = 0$ and $M = 0$.

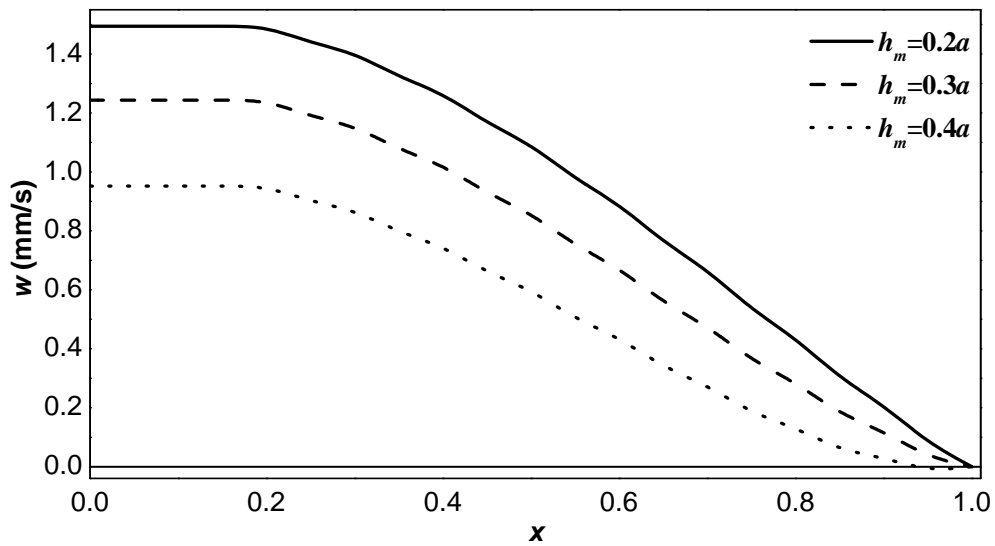


Fig. (3). Axial velocity .vs. x for different stenosis height h_m at $z=0.036m$, $ng = 6$, $\phi = \pi/4$, $M = 0$.

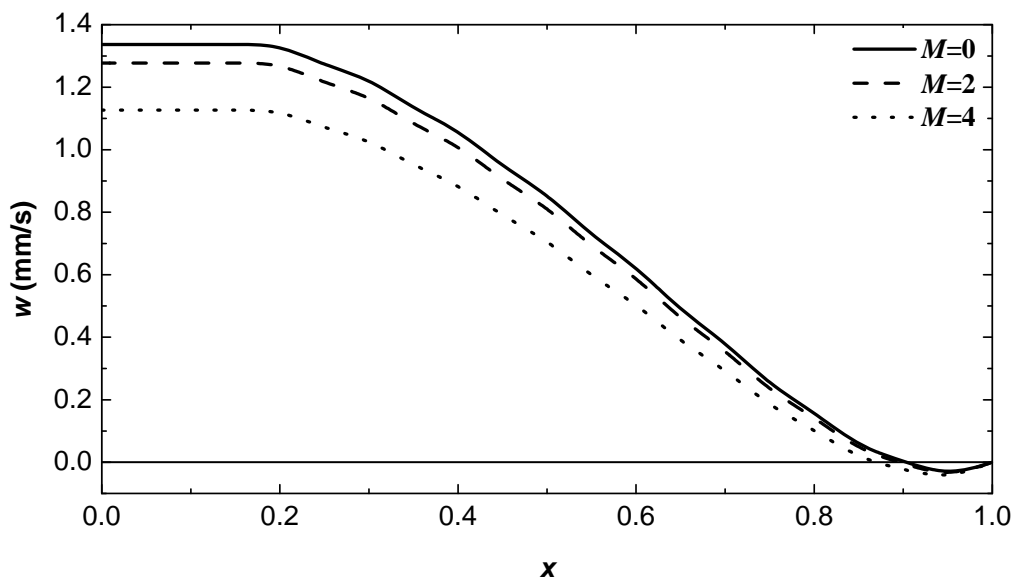


Fig. (4). Axial velocity .vs. x for different value of M at $z = 0.036m$ for $\phi = \pi/4$, $h_m = 0.4a$, $ng = 6$.

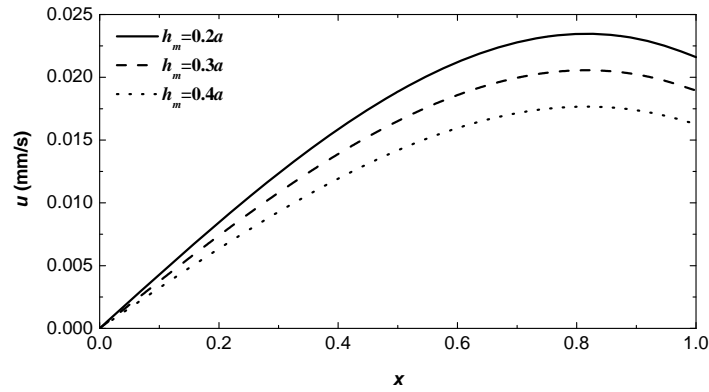


Fig. (5). Radial velocity vs. x for different stenosis height h_m at $z = 0.036\text{m}$, $ng = 6$, $\phi = \pi/4$, $M = 0$.

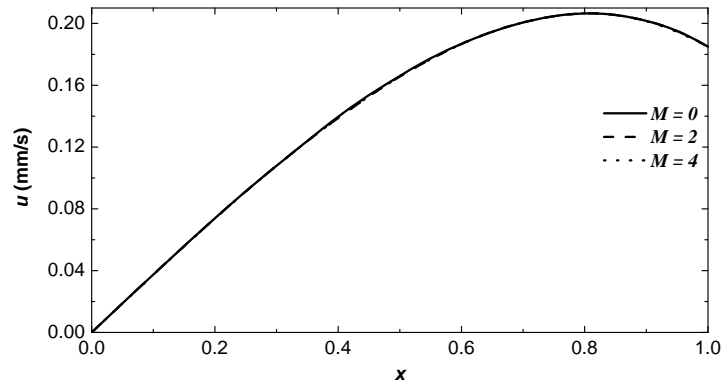


Fig. (6). Radial velocity vs. x for different value of M at $z = 0.0336\text{m}$ for $\phi = \pi/4$, $h_m = 0.4a$, $ng = 2$.

1060 Kg/m^3 , $\text{Re} = 300$. The length of the artery is considered 0.06 m . Also, the range of the some other parameters are $\phi [0, \pi]$, $ng [2, 6]$, $M [0, 4]$ and $\tau_y [0, 0.0033]$.

An explicit finite difference scheme which was used in Ikbal *et al.* [32] is applied here also, to solve the resulting equations along with the boundary conditions and the results are observed to converge with an accuracy of order 10^{-5} , for the time step 0.00001 . To achieve the desired accuracy of the result, we considered the mesh containing the grid 60×40 . The computation code based on the following algorithm has been successfully programmed using C-language. The algorithm is presented below in terms of the variables used in the equations:

- i. Set the initial velocity profile as given in the equation (39.a) for the problem with magnetic field and as given in the equation (39.b) for the problem in the absence of the magnetic field at the entire domain.
- ii. Calculate $w_{i,j}^{k+1}$ at the next instant of the time t_1 ($t_1 = t_0 + dt$) from equation (36) by making use of equation (37), along with the boundary conditions (38). The relation of the pressure gradient is used from the equation (14).
- iii. Calculate $u_{i,j}^{k+1}$ at t_1 using the computed axial velocity $w_{i,j}^{k+1}$ from the equation (34).
- iv. Computation for $t = t_1$ are continued throughout the whole domain.

- v. The above sequences of steps are repeated for the next time increment and continue until the solution at the desired time step has been achieved.

Using these radial and axial velocities, the wall shear stress and the volumetric flow at different axial locations is calculated and these values are tabulated and plotted in this section for different value of the physical parameters. To ascertain the accuracy of the present results, a comparison is made with the results given in Mandal *et al.* [30] for axial velocity and for Newtonian fluid which is shown in Fig. (2). The axial and radial velocities, wall shear and the volumetric flow rate are obtained for a wide range of parameters such as the asymmetry parameter, the height of the stenosis, phase angle, Hartmann number and are presented below through (Figs. 3 to 12). Some of important results are tabulated through Tables 1 to 4 Increase in the height of the asymmetric stenosis, the artery becomes very narrow and because of this, a back flow is noticed for some values of h_m . One such case is shown in Fig. (3) which clearly shows a reduction in the axial velocity as h_m increases, and it also decreases with the radial distance. A close examination reveals that for the asymmetric stenosis, with $ng = 6$, a back flow is seen at the axial position $z = 0.036\text{m}$, for $h_m = 0.4a$. Also, the effect of the magnetic parameter M increased the intensity and span of this back flow which is shown in Fig. (4).

In Fig. (5), the radial velocity profile plotted against different heights of the stenosis, in the absence of the magnetic field at a particular position $z = 0.036\text{m}$ of the artery and at a particular instant of time, $t = 4\text{s}$. With increase in the height of the stenosis, the radial velocity also decreased. The radial velocity increased along the radial direction up to a

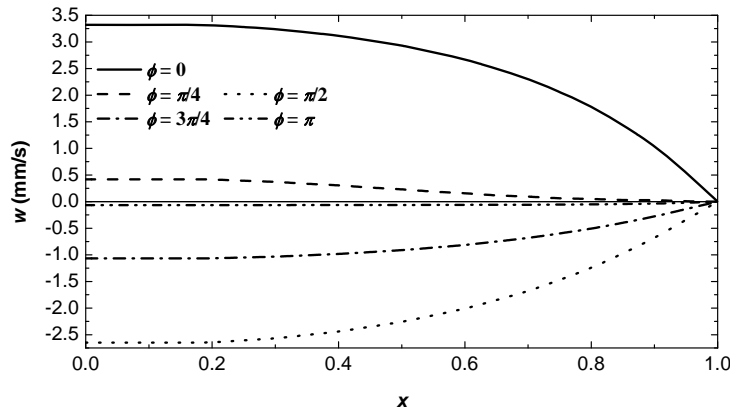


Fig. (7). Axial velocity vs. x for phase angle ϕ at $z=0.0336m$, $ng = 2$, $h_m = 0.4a$, $M = 0$.

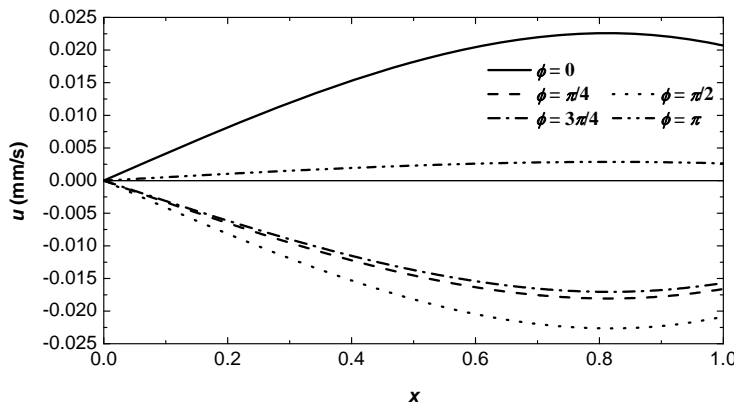


Fig. (8). Radial velocity vs. x for phase angle ϕ at $z = 0.0336m$, $ng = 2$, $h_m = 0.4a$, $M = 0$.

point near the wall, after which it decreased due to moving wall boundary condition at the wall. The effect of magnetic parameter is not much significant on the radial velocity, this can be noticed from Fig. (6) which is plotted for the case of symmetric stenosis.

The effect of the phase angle of the externally imposed body acceleration on the flow field is shown in (Figs. 7 and 8). Due to the change in the phase angle, the external body forces changes and this has a significant effect on the flow characteristics. Several plots have been made in (Fig. 7), to characterize the axial velocity at a specific location $z = 0.0336m$, of the symmetric (i.e., $ng = 2$) stenosed artery, for Reynolds number $Re = 300$ at instant $t = 4s$. A backflow occurs for the cases $\phi = \pi / 2$, $3\pi / 4$ and π . For all the cases the velocity profile is of parabolic nature, the absolute value of the axial velocity start from its maximum at the axis and then it decreases and finally reaches to zero at the wall to follow the no-slip condition. The velocity maximum is achieved for the case $\phi = 0$.

The radial velocity is calculated for different phase angles at a specific location $z = 0.0336 m$, at the instant $t = 4s$. From the Fig. 8, it is observed that the radial velocity profiles are totally negative for $\phi = \pi / 4, \pi / 2$ and $3\pi / 4$ while the nature of all these curves is same. All the curves initially start from zero and their magnitude increases with the axis and finally reach a maximum value near the artery wall and then decreases a little and attain the wall velocity. The pro-

files are positive for the values $\phi = 0$ and π . There is a little difference in the velocity profiles between $\phi = \pi / 4$ and $\phi = 3\pi / 4$. The velocity is maximum for $\phi = 0$ and for $\phi = \pi / 2$, is minimum and completely negative.

The presence of the stenosis, restricts the flow of blood in the narrow artery, which leads to variations in the wall shear. The wall shear for different geometric parameter (ng) is shown in Fig. (9a), which is plotted for $t = 4s$ with phase angle $\phi = \pi / 4$, $h_m = 0.4a$ in the absence of magnetic field. It is worth mentioning that the starting point of the stenosis is $z = 0.025m$ and its length is $l = 0.015m$. These numbers are same for the asymmetric stenosis also. From the Fig. (9a) it is evident that there is a region both before and after the stenosis where the change in the wall shear is seen for both the symmetric and asymmetric stenosis. Sharp symmetric peaks are seen about the axis of the flow for the case of the symmetric stenosis. It is interesting to note that the change in the wall shear is symmetric for the case of symmetric stenosis and is asymmetric for the asymmetric one. For the case of asymmetric stenosis, the wall shear curve is flat for the pre peak position of the stenosis while a sharp peak is noticed near the peak of this asymmetric stenosis. This character becomes more prominent as the value of ng increases. Also, a comparison is made with the Newtonian fluid wall shear stress for both the symmetric and asymmetric ones in (Figs. 9b and 9c). These plots show similar behavior as mentioned above for the Newtonian fluid structure also, while the wall shear is more for the Casson fluid than the Newtonian fluid.

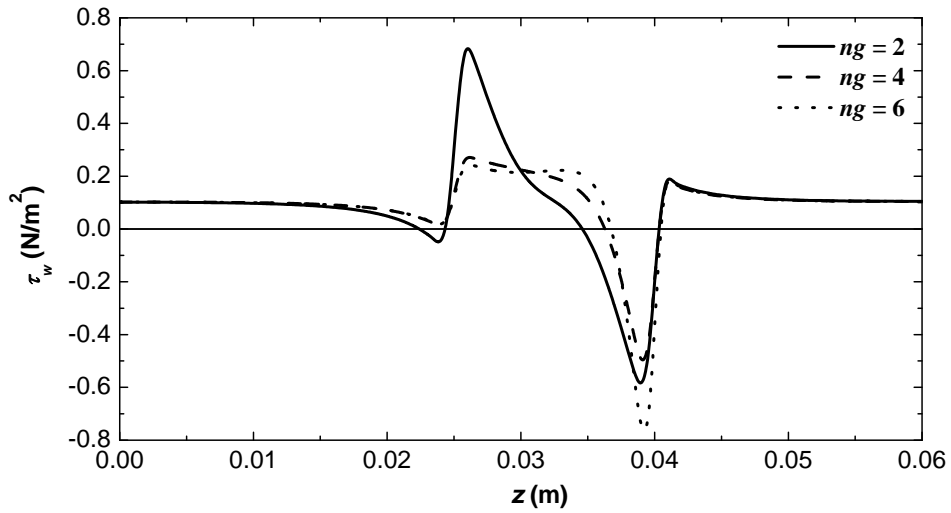


Fig. (9a). Wall Shear vs. z for different geometric parameter ng with phase angle $\phi = \pi/4$, $h_m = 0.4a$, $M = 0$.

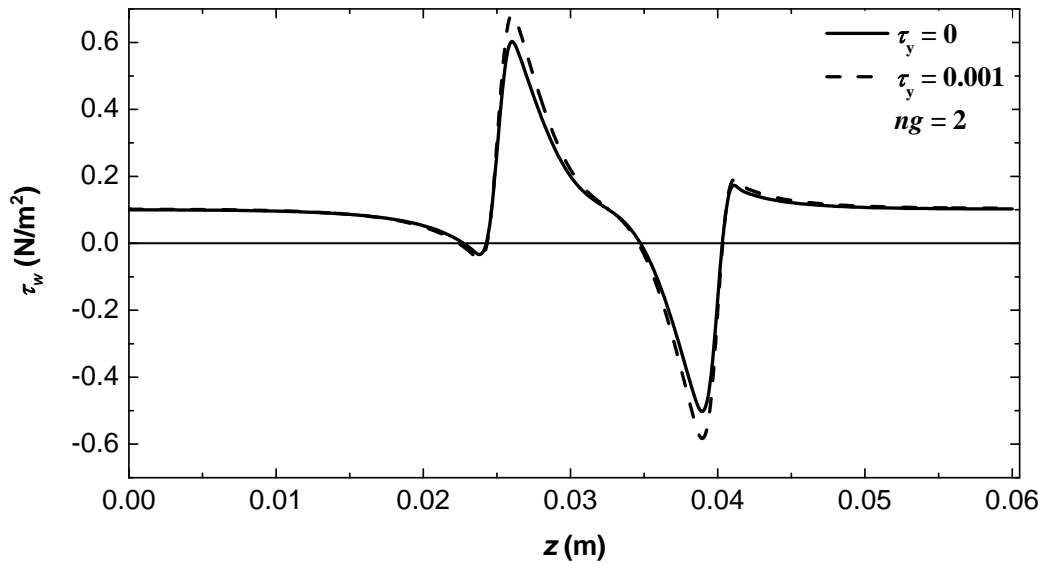


Fig. (9b). Wall Shear vs. z for different τ_y with $ng = 2$, phase angle $\phi = \pi/4$, $h_m = 0.4$, $M = 0$.

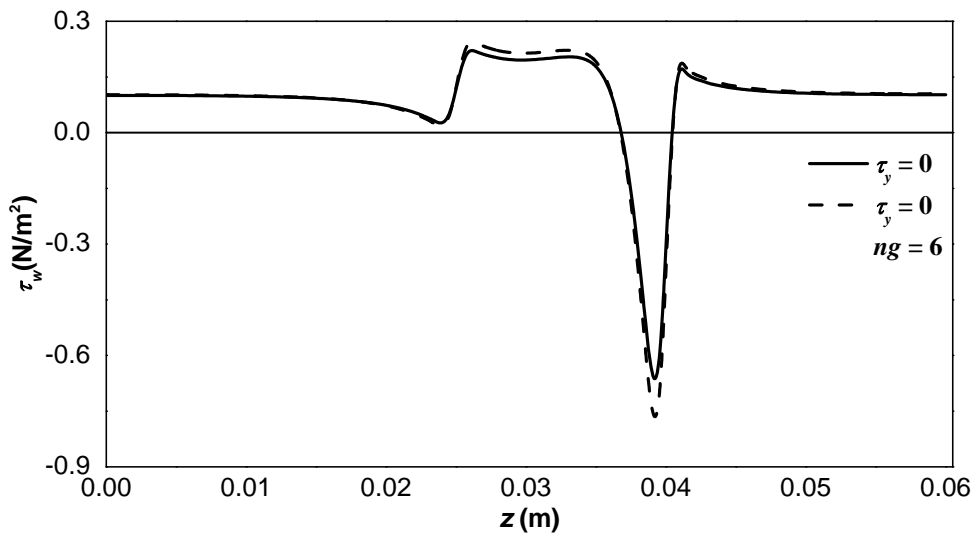


Fig. (9c). Wall Shear vs. z for different τ_y with $ng = 6$, phase angle $\phi = \pi/4$, $h_m = 0.4a$, $M = 0$.

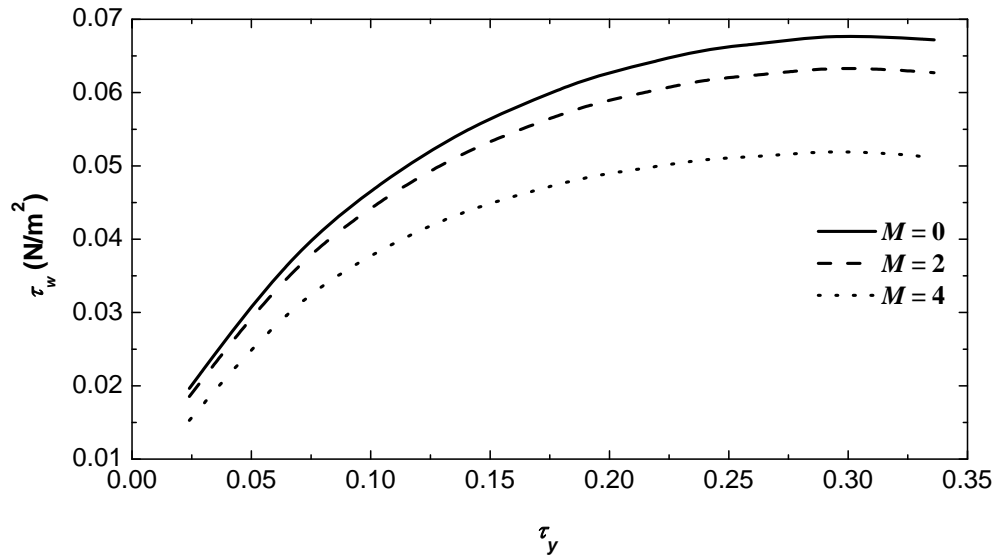


Fig. (10a). Wall Shear vs. yield stress τ_y for different M at $z = 0.0336m$ with $ng = 2$, $\varphi = \pi/4$, $h_m = 0.4a$.

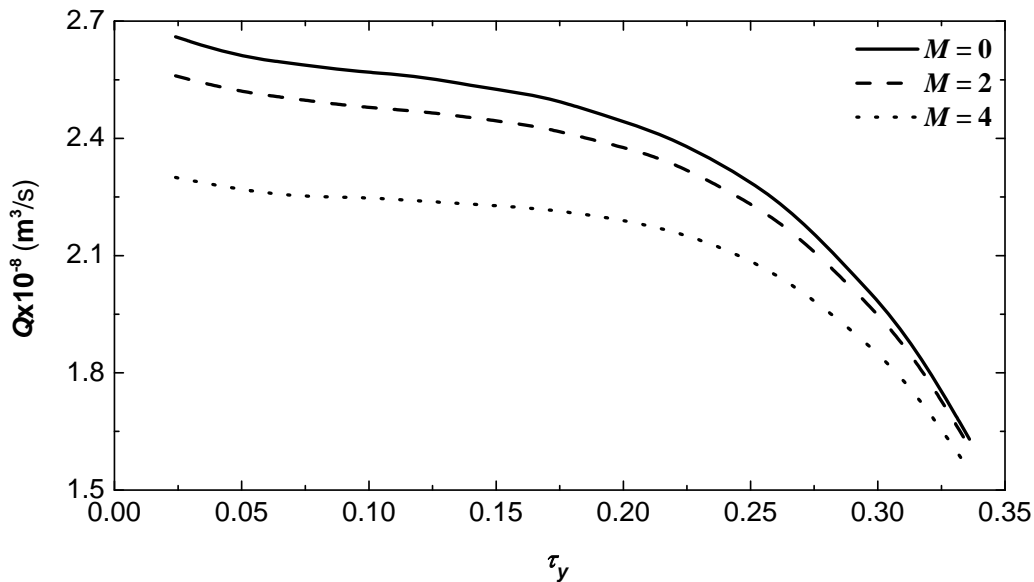


Fig. (10b). Volumetric flow Q vs. yield stress τ_y at different M at $z = 0.0336m$ with $\varphi = 0$, $h_m = 0.4a$, $ng = 2$.

The volumetric flow and the wall shear are calculated using the formulae given in equation (40 - 41), its variation against the yield stress is plotted in (Figs. 10 and 11) for different values of the Hartmann number and the phase parameter of the body acceleration. The wall shear is increasing with increase in the Hartmann number. This feature is shown for the symmetric stenosis in the (Fig. 10a). Also, the wall shear is increasing non-linearly with the yield stress parameter. From the (Fig. 10b), it is evident that the volumetric flow decreases with the Hartmann number, and also with the yield stress parameter. A close observation of this figure indicate that with the increase in the Hartmann number there is a significant reduction in the volumetric flow rate, and this reduction increases with the increase in the phase of the body acceleration parameter, this is also noticeable from (Fig. 11a). Variation of the volumetric flow and wall shear for different values of phase parameter of the body acceleration is plotted in (Figs. 11a and 11b) indicate that there is intense backflow in the tube near the peak of the stenosis.

A substantial reduction is noticed for the volumetric flow rate as the height of the stenosis increases, this is shown for different values of height of the symmetric stenosis in (Fig. 12a). A substantial increment is noticed for wall shear as the height of the stenosis increases and this is shown in (Fig. 12b).

The radial and axial velocities for three different values of the asymmetry parameter ng of the stenosis is tabulated at the pre stenosis, peak of the stenosis and post stenosis positions (the value of the axial position is indicated therein) of the artery at different radial locations. It is worth mentioning that the peak of the stenosis changes with the value of the asymmetry parameter. From the Table 1, it is clear that the radial velocity is same for the pre and post stenosis positions while it is different at the peak of the stenosis in all the three cases considered. This can be seen from the equation (34). The expression for R is independent of z for the pre and post stenosis positions, hence the radial velocity remains a con-

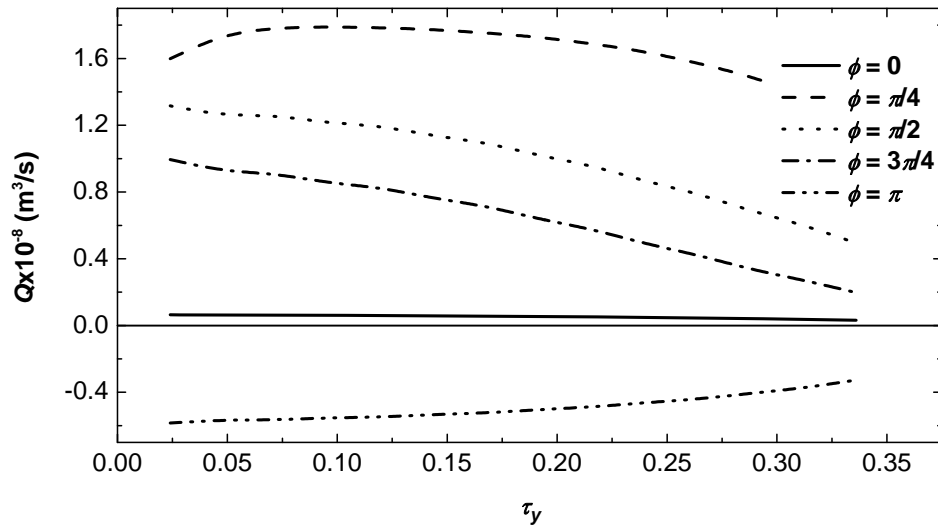


Fig. (11a). Volumetric flow Q vs. yield stress τ_y for different ϕ at $z = 0.0336\text{m}$ with $h_m = 0.2a$, $\phi = \pi/4$, $M = 0$, $ng = 2$.

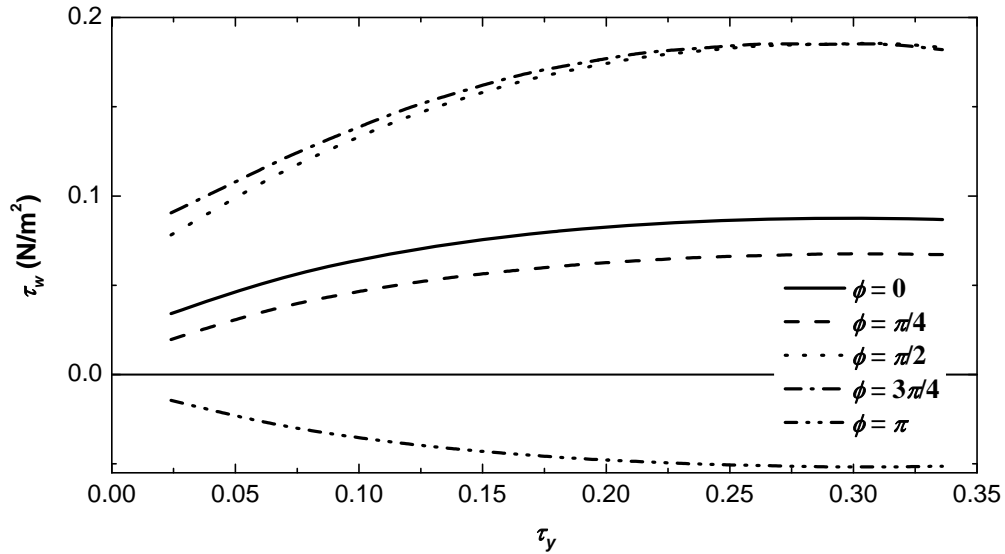


Fig. (11b). Wall Shear vs. yield stress τ_y for different phase angle ϕ at $z = 0.0336\text{m}$ with $h_m = 0.4a$, $ng = 2$, $M = 0$.

Table 1. Radial Velocity vs. x for Different Position of z and $ng = 2, 4, 6$ with $\phi = \pi/4$, $h_m = 0.4a$, $M = 0$

u x	Pre			Peak			Post		
	ng=2 z=0.024 (m)	ng=4 z=0.024 (m)	ng=6 z=0.024 (m)	ng=2 z=0.033 (m)	ng=4 z=0.0348 (m)	ng=6 z=0.036 (m)	ng=2 z=0.042 (m)	ng=4 z=0.042 (m)	ng=6 z=0.042 (m)
0.2	0.010536	0.010536	0.010536	0.006464	0.007920	0.007658	0.010563	0.010563	0.010563
0.4	0.019834	0.019834	0.019834	0.012140	0.014871	0.014381	0.019834	0.019834	0.019834
0.6	0.026517	0.026517	0.026517	0.016233	0.019881	0.019228	0.026517	0.026517	0.026517
0.8	0.029320	0.029320	0.029320	0.017934	0.021976	0.021251	0.029320	0.029320	0.029320
1.0	0.026948	0.026948	0.026948	0.016401	0.020177	0.019474	0.026948	0.026948	0.026948

stant for a fixed x and time t . Since R depends on z for the stenosis region, the radial velocity varies with the axial distance.

It can be seen from the Table 2, that the axial velocity increases with the axial distance from the pre stenosis region to post stenosis region. It decreased with the non-dimensional

Table 3. Volumetric Flow Q vs. Yield Stress τ_y at Different Position z for $ng = 2, 4, 6$ with $\phi = \pi/4, h_m = 0.4a$

$Q \times 10^{-8}$ (m^3/s) τ_y	Pre			Peak			Post		
	ng=2 z=0.024 (m)	ng=4 z=0.024 (m)	ng=6 z=0.024 (m)	ng=2 z=0.033 (m)	ng=4 z=0.0348 (m)	ng=6 z=0.036 (m)	ng=2 z=0.042 (m)	ng=4 z=0.042 (m)	ng=6 z=0.042 (m)
0.00024	-0.2125	0.14653	0.329308	0.495661	0.863551	0.652556	2.945853	2.657284	2.657585
0.00096	-0.3319	0.019384	0.200052	0.458874	0.790123	0.579173	2.880234	2.562264	2.562372
0.00168	-0.5372	-0.21277	-0.01892	0.413276	0.68534	0.459611	2.852723	2.472158	2.467795
0.0024	-0.8913	-0.63586	-0.42761	0.31723	0.470337	0.218112	2.732478	2.242174	2.227446
0.00312	-1.0383	-0.92308	-0.71808	0.210706	0.258673	0.005142	2.303048	1.790533	1.762

Table 4. Wall Shear vs. Yield Stress τ_y at Different Position for $ng = 2, 4, 6$ with $M = 0, \phi = \pi/4, h_m = 0.4a$

τ_w (N/m^2) τ_y	Pre			Peak			Post		
	ng=2 z=0.024 (m)	ng=4 z=0.024 (m)	ng=6 z=0.024 (m)	ng=2 z=0.033 (m)	ng=4 z=0.0348 (m)	ng=6 z=0.036 (m)	ng=2 z=0.042 (m)	ng=4 z=0.042 (m)	ng=6 z=0.042 (m)
0.00024	2.30305	1.79053	1.762	0.21071	0.25867	0.00514	-1.03827	-0.7180	-0.9230
0.00096	2.73248	2.24217	2.22745	0.31723	0.47034	0.21811	-0.8913	-0.4276	-0.6358
0.00168	2.85272	2.47216	2.4678	0.41328	0.68534	0.45961	-0.53724	-0.0189	-0.2127
0.0024	2.88023	2.56226	2.56237	0.45887	0.79012	0.57917	-0.33185	0.20005	0.01938
0.00312	2.94585	2.65728	2.65759	0.49566	0.86355	0.65256	-0.21251	0.32931	0.14653

radial position in all the regions. It also indicates that there exists a back flow for the case of symmetric stenosis near the pre-stenosis region while this back flow disappears as the value of the asymmetry parameter ng is increased. This is because of the favorable pressure gradient develops near the wall with the increase in the value of ng .

Tables 3 and 4 give a detailed description about the volumetric flow rate and the wall shear against the yield stress parameter at the three different positions for the three types of stenoses considered in the present investigation, the description of which is already presented in the corresponding figures.

CONCLUSION

The present analysis investigates the effect of the magnetic field and externally imposed body acceleration on the blood flow (Casson model) in the presence of asymmetric stenosis in an arterial segment. Results indicate that the magnetic field (M), yield stress (τ_y), phase angle (ϕ) and the geometric parameter of the stenosis (ng) have significant effect on the flow characteristics. With the increase in the strength of the magnetic field, both the radial and axial velocities decreased. In all the cases a back flow occurs at the upstream zone of the constricted site. The recirculation zone increases in the upstream position of the stenosis with the geometric parameter. Due to body acceleration, the flow

characteristics change drastically. Flow reversal is seen for the phase angles (ϕ) $\pi/2, 3\pi/4$ and π . With the narrowing of the constricted zone (increasing the height of the stenosis), both the axial and radial velocities decreased. A sudden fall in wall shear is noticed at the starting point of the stenosis due to the formation of vorticity which occur at the upstream position of the stenosis. Increase in the value of yield stress reduced the volumetric flow. The value of the wall shear stress increases with increase in the value of yield stress. Thus, the flow field and the volumetric flow are significantly affected due to the body acceleration term.

ACKNOWLEDGMENTS

The authors are thankful to the reviewers for advising us on the important technical points. The first author is thankful to the CSIR India for the financial support provided for carrying out this work through S R F; (CSIR F. No. 10-2(5)/2004(II)-E.U. II).

NOMENCLATURE

- a_0 = amplitude of the body acceleration
- A_0 = the steady state part of the pressure gradient

A_1	=	the amplitude of its oscillating part of pressure gradient
B_0	=	external magnetic field
B_1	=	the induced magnetic field
d	=	distance of the stenosis from the inlet
E	=	the electric field
f_b	=	frequency of body acceleration
f_p	=	being the heart pulse frequency
h_m	=	the maximum height of the stenosis
I_0	=	modified Bessel function of the first kind of order zero
J	=	the current density
l	=	the length of the stenosis
M	=	Hartmann number
ng	=	the parameter representing the asymmetry of the stenosis
r_0	=	the unstricted radius of the stenosed vessel
p	=	pressure
Re	=	Reynolds number
$u(r,z,t)$	=	radial components of the velocity
$w(r,z,t)$	=	the axial velocity
W_0	=	the average velocity at the axial direction

Greek Symbol

η	=	the shape of the stenosis
ϕ	=	phase angle
σ	=	electrical conductivity
τ_y	=	yield stress
k_c^2	=	apparent viscosity
δ_{ij}	=	Kronecker delta
τ_{ij}	=	stress component
v_{ij}	=	the shear rate
Δx	=	increment at the axial direction
Δz	=	increment radial direction
Δt	=	increment in time step

REFERENCES

[1] D. A. McDonald. *Blood flow in arteries*; 2nd ed, Edward Arnold: London, 1974.
 [2] W. R. Milnor. *Hemodynamics*" Williams and Williams: Baltimore, 1982.

[3] T. J. Pedley. *The fluid mechanics of Large Blood Vessels*", Cambridge University Press: Cambridge, 1980.
 [4] B. Pincombe, J. Majumder, and J. H. Craig, "Effect of multiple stenoses and post stenotic dilation on non-Newtonian blood flow in small arteries". *Medical Biology and Engineering Computation*, vol. 37, pp. 595-599, 1999.
 [5] D. S. Sankar, and Usha Lee. "Two fluid non-Linear models for flow in catheterized blood vessels", *International Journal of Non-Linear Mechanics*, vol. 43, pp. 622-631, 2008.
 [6] S. Chakravarty and P. K. Mandal, "A non-linear two dimensional model of blood flow in an overlapping arterial stenosis subjected to body acceleration", *Mathematics and Computer Modeling*, vol. 24, pp. 43-58, 1996.
 [7] S. Chakravarty and P. K. Mandal, "Two dimensional blood flows through tapered arteries under stenosis conditions", *International Journal of Non-Linear Mechanics*, vol. 35, pp. 779-793, 2000.
 [8] S. Chakravarty, P. K. Mandal and Sarifuddin, "Effect of surface irregularities on unsteady pulsatile flow in a compliant artery", *International Journal of Non-Linear Mechanics*, vol. 40, pp. 1268-1281, 2005.
 [9] G. A. Johnson, H. S. Borovertz and J. I. Anderson, "A model of pulsatile flow in a uniform deformable vessel", *Journal of Biomechanics*, vol. 25, pp. 91-100, 1992.
 [10] S. Chakravarty and P.K. Mandal, an analysis of pulsatile flow in a model aortic bifurcation", *International Journal of Engineering Science*, vol. 35, no. 4, pp. 409-422, 1997.
 [11] Y. C. Fung, "*Biomechanics: Mechanical properties of Living Tissues*". Spring, Berlin, 1981.
 [12] J. Aroesty and J. F. Gross, "The mechanics of the pulsatile flow in small vessel – I: Casson theory", *Microvascular Research*, vol. 4, pp. 1-12, 1972.
 [13] S. E. Charm and G. S. Kurland, "Viscometry of human blood for small rates of 0-100,000". *Nature*, vol. 206, p. 617, 1965.
 [14] P. Chaturani and R. P. Samy, "Pulsatile flow of a Casson fluid through stenosed arteries with application to blood flow", *Biorheology*, vol. 23, pp. 499-510, 1986.
 [15] Bigyani Das and R. L. Batra, "Secondary flow of a Casson fluid in a slightly curved tube", *International Journal of Non-Linear Mechanics*, vol. 28, pp. 567-577, 1993.
 [16] R. K. Dash and K. N. Mehta, "Cason fluid flow in a pipe filled with a homogeneous porous medium", *International Journal of Engineering Science*, vol. 34, pp. 1145-1156, 1996.
 [17] P. Nagarani, G. Sarojamma and G. Jayaraman, "Effect of boundary absorption in dispersion in Casson fluid flow in a tube", *Annals of Biomedical Engineering*, vol. 32, pp. 706-719, 2004.
 [18] K. Rohlf, "the role of the Womersley number in pulsatile blood flow a theoretical study of the Casson model", *Journal of Biomechanics*, vol. 34, pp. 141-148, 1996.
 [19] P. A. Voltairas, D. I. Fotiadis and L. K. Michalis, Hydrodynamics of magnetic drug targeting, *Journal of Biomechanics*, vol. 35, pp. 813-821, 2002.
 [20] Y. Haik, V. Pai and C. J. Chen, "Development of magnetic device for cell separation. *Journal of Magnetism and Magnetic Material*", vol. 194, pp. 254-261, 1999.
 [21] S. Bhargava, S. Rawat, H. S. Takhar and O. A. Beg, "Pulsatile magneto-biofluid flow and mass transfer in a non-Darcian porous medium channel", *Meccanica*, vol. 42, pp. 247-262, 2007.
 [22] R. Bhargava, H.S. Sugandha, S. Rawat, K. Halim and H. S. Takhar, "Computational modeling of biomagnetic micropolar blood flow in porous medium", *Journal of Biomechanics*, vol. 39, pp. S648-S649, 2006.
 [23] Sasa Kenjeres, "Numerical analysis of blood flow in realistic arteries subjected to strong non-uniform magnetic field", *International Journal of Heat and Fluid flow*, vol. 29, pp. 752-764, 2008.
 [24] C. Midya, G. C. Layek and A. S. Gupta, "Magneto-hydrodynamic viscous flow separation in a channel with constrictions", *ASME Journal of Engineering*, vol. 125, pp. 952-962, 2003.
 [25] E. E. Tzirtzilakis, "A mathematical model for blood flow in magnetic field", *Physics of Fluids*, vol. 17, pp. 103-115, 2005.
 [26] E. E. Tzirtzilakis, "Biomagnetic fluid flow in a channel with stenosis", *Physica D*, vol. 237, pp. 66-81, 2008.
 [27] S. Ichioka, M. Minegishi, M. Iwasaka, M. Shibata, T. Nakatsuka, K. Harii, A. Kamiya, and S. Ueno, "High-intensity static magnetic fields modulate skin microcirculation and temperature *in vivo*", *Bioelectromagnetics* (N.Y.) vol. 21, pp. 183-188, 2000.

- [28] O.A. Beg, R. Bhargava, S. Rawat, K. Halim, and H.S. Takhar, "Computational modeling of biomagnetic micropolar blood flow and heat transfer in a two-dimensional non-Darcian porous medium", *Meccanica*, vol. 43, pp. 391-410, 2008.
- [29] Y. Haik, C.J. Chen, and J. Chatterjee. "Numerical simulation of biomagnetic fluid in a channel with thrombus, *Journal of Visualization* , vol. 5, no. 2, pp. 187-195, 2002.
- [30] P. K. Mondal, S. Chakravarty, and A. "Mondal. Effect of body acceleration on unsteady pulsatile flow of non-Newtonian fluid through a stenosed artery", *Applied Mathematics and Computation*, vol. 189, pp. 766-779, 2007.
- [31] D. S. Sankar, and Usik Lee. "Mathematical modeling of pulsatile flow of non-Newtonian fluid in stenosed arteries", *Communication in Non-Linear Science and Numerical Simulation*, vol. 14, pp. 2971-2981, 2009.
- [32] Md. A. Iqbal, S. Chakravarty, Kelvin K. L. and Wong, J. Mazumdar, and P. K. Mandal, "Unsteady response of non-newtonian blood flow through a stenosed artery in magnetic field", *Journal of Computational and Applied Mathematics*, vol. 230, pp. 243-259, 2009.

Received: July 01, 2009

Revised: October 29, 2009

Accepted: October 30, 2009

Shaw et al.; Licensee Bentham Open.

This is an open access article licensed under the terms of the Creative Commons

© Attribution Non-Commercial License (<http://creativecommons.org/licenses/by-nc/3.0/>) which permits unrestricted, non-commercial use, distribution and reproduction in any medium, provided the work is properly cited.